Pattern selection in binary-fluid convection at positive separation ratios

E. Knobloch*
Department of Physics, Kyoto University, Kyoto 606, Japan
(Received 28 November 1988)

Pattern selection in binary-fluid mixtures heated from below is studied for separation ratios S in the regime $0 < S_\infty - S \ll 1$, where S_∞ is the critical value for which the wavelength $2\pi/k_c$ of the instability first becomes infinite. The basic equations are reduced to a scalar equation for the horizontal planform whose coefficients can be determined analytically for boundary conditions of experimental interest. Equivariant bifurcation theory is used to study pattern selection on both square and hexagonal lattices. The results depend strongly on the parameter β describing asymmetry in the boundary conditions at top and bottom. When $\beta=0$, squares are stable on the square lattice but are replaced by rolls with increasing β. The transition between stable squares and stable rolls takes place via a stable branch of new solutions called crossrolls. On the hexagonal lattice, hexagons are stable if $\beta=0$, but rolls are stable when $\beta\neq 0$.

I. INTRODUCTION

Some time ago Le Gal *et al.*[1] reported the results of a large-aspect-ratio convection experiment in which they saw the initial instability develop into a pattern of squares. With increasing Rayleigh number the squares lost stability to an oscillation between two roll patterns at right angles; with further increase these oscillations were superseded by a time-independent roll pattern. These phenomena were subsequently attributed to the multicomponent nature of the fluid used[2] and similar behavior was observed in a binary-fluid mixture.[2] However, a detailed explanation of the experimental observations is still unavailable. A rigorous bifurcation analysis near a steady-state bifurcation in a binary fluid with idealized boundary conditions found no stable squares.[3] A more heuristic approach in which a set of modes was selected to satisfy the crucial no-mass-flux boundary condition was able to identify stable squares but only after *ad hoc* side-wall forcing was incorporated.[4] In the present paper we develop an exact theory in which all the experimental boundary conditions are satisfied and rigorous bifurcation analysis can be carried out analytically. To do all this we select the parameter region rather carefully. We note that owing to the no-mass-flux boundary condition, the wave number of the mode that first becomes unstable will vanish if the separation ratio S exceeds a critical value S_∞.[5,6] For values of S such that $0 < S_\infty - S \ll 1$, the wave number is finite but small. It is therefore possible to take advantage of the smallness of the critical wave number to introduce a small parameter into the hydrodynamical equations. The method follows the basic idea developed by Chapman and Proctor and Gertsberg and Sivashinsky for pure fluids,[7-10] and yields an evolution equation for the horizontal planform of the instability that is much simpler than the original fluid equations. In particular all the intricacies of the boundary conditions are absorbed into a few coefficients that appear in this equation. We calculate these coefficients for a variety of velocity and thermal boundary conditions at the top and bottom of the fluid layer and use the results to calculate S_∞ analytically for each case. In addition, we find that the boundary conditions influence the structure of the nonlinear terms in the evolution equation. Specifically, we distinguish between boundary conditions that are symmetric at the top and bottom and those that are not, and derive evolution equations that are characteristic of these two cases. We find that the behavior of both equations is captured by a particular problem in which the boundary conditions at the top and bottom plates differ only slightly.

The analysis of pattern selection follows in the spirit of earlier studies. The problem is formulated on a doubly periodic lattice, and the techniques of equivariant bifurcation theory are used to determine the relative stability of the various patterns that lie on the square and hexagonal lattices.[11] Since the evolution equation is similar to another one studied at length by the author,[12] many of the mathematical details are omitted from the present paper. We find that on the square lattice, squares are indeed preferred provided the boundary conditions at the top and bottom are sufficiently alike, as hypothesized in Ref. 2. However, when the boundary conditions are sufficiently different, in a sense described below, rolls are preferred. In particular, if the terms representing this effect are present, squares will be replaced by rolls as S approaches S_∞. We show, by analyzing a particular codimension-two bifurcation, that with increasing Rayleigh number stability is transferred from the rolls back to the squares via a stable branch of solutions called cross rolls.

A parallel study of the hexagonal lattice is also presented. Here it is necessary to distinguish between the "symmetric" problem with identical boundary conditions at the top and bottom, and the "nonsymmetric" problem. The former is found to be always degenerate in that a particular nonlinear term in the bifurcation equations vanishes identically.[12] As a consequence, there are as many as six possible primary solution branches that bifurcate from the trivial solution at criticality. We calcu-

late the necessary fifth-order terms and apply existing analysis of this degeneracy[12] to conclude that hexagons are stable. In the nonsymmetric problem, four solution branches bifurcate simultaneously and of these, rolls are stable. Thus the hexagons lose stability as soon as the boundary conditions at top and bottom become different.

The paper is organized as follows. In Sec. II the evolution equation is derived. The square and hexagonal lattices are studied in Secs. III and IV, respectively. The results are summarized and discussed in Sec. V.

II. DERIVATION OF THE EVOLUTION EQUATION

Suitably nondimensionalized, the equations describing two-dimensional Boussinesq convection in a binary-fluid mixture heated from below take the form[13]

$$\frac{1}{\sigma}\left[\frac{\partial}{\partial t}\nabla^2\psi+J(\psi,\nabla^2\psi)\right]=R(1+S)\theta_x+SR\phi_x+\nabla^4\psi\ , \tag{2.1a}$$

$$\frac{\partial\theta}{\partial t}+J(\psi,\theta)=\psi_x+\nabla^2\theta\ , \tag{2.1b}$$

$$\frac{\partial\phi}{\partial t}+J(\psi,\phi)=\tau\nabla^2\phi-\nabla^2\theta\ , \tag{2.1c}$$

where $\psi(x,z,t)$ is the stream function, $\theta(x,z,t)$ denotes the departure of the temperature from its conduction profile, and $\phi(x,z,t)=\Sigma-\theta$, where $\Sigma(x,z,t)$ is the similarly defined concentration distribution. There are four dimensionless parameters, the Prandtl number σ, the Lewis number τ, the separation ratio S, and the Rayleigh number R. Finally, the symbol $J(f,g)$ denotes the Jacobian $f_xg_z-f_zg_x$.

As boundary conditions we impose the no-mass-flux condition

$$D\phi=0 \quad \text{on } z=\pm1\ , \tag{2.2}$$

where $D\equiv\partial/\partial z$, and consider the following possibilities for the stream function ψ and the temperature θ:

$$\psi=D^2\psi=0 \quad \text{on } z=\pm1\ , \tag{2.3a}$$

$$\psi=D\psi=0 \quad \text{on } z=\pm1\ , \tag{2.3b}$$

$$\psi=D^2\psi=0 \quad \text{on } z=1\ ,\qquad \psi=D\psi=0 \quad \text{on } z=-1\ , \tag{2.3c}$$

$$\theta=0 \quad \text{on } z=\pm1\ , \tag{2.3d}$$

$$\theta=0 \quad \text{on } z=1\ ,\qquad D\theta=0 \quad \text{on } z=-1\ . \tag{2.3e}$$

These conditions state that the boundaries $z=\pm1$ are streamlines ($\psi=0$), either stress-free ($D^2\psi=0$) or no-slip ($D\psi=0$), and that the temperature is held constant ($\theta=0$) or that heat is supplied at a constant rate ($D\theta=0$). We do not consider here the case

$$D\theta=0 \quad \text{on } z=\pm1 \tag{2.3f}$$

corresponding to thermally insulating boundaries at both top and bottom.[10] Note that we have imposed boundary conditions at $z=\pm1$ instead of the more usual $z=1,0$. The present choice, however, allows us to take advantage of certain symmetries inherent in the problem, as explained further below.

Equations (2.1) have the trivial solution $\psi=\theta=\phi=0$, corresponding to no motion. As the rate of heating, measured by the Rayleigh number R, is increased, this state loses stability and convection sets in. For sufficiently large positive separation ratios S, the wavelength of the mode that first becomes unstable is infinite. This behavior, studied in detail in Ref. 6, arises because the separation caused by a destabilizing temperature gradient becomes so effective at setting up an additional destabilizing concentration gradient that the stability of the system is essentially controlled by the latter. Because of the no-mass-flux boundary condition, the system behaves as a pure Rayleigh-Bénard convection with fixed thermal flux boundary conditions for which the wave number of the mode that first loses stability is well known to vanish.[14] This occurs because, for example, the fluid near the top boundary does not lose heat to the boundary and so does not cool and descend. Since heat is still exchanged between up-welling and down-welling motions rendering heat transport less efficient, long wavelengths are favored. The same explanation applies to the no-mass-flux problem.

In the following we take advantage of the long wavelength of the initial instability, and introduce the following slow variables:[7]

$$x=X/\epsilon,\quad t=T/\epsilon^4,\quad 0<\epsilon\ll1\ . \tag{2.4}$$

In addition we scale

$$\psi=\epsilon\Psi(X,z,T),\quad \theta=\epsilon^2\Theta(X,z,T),\quad \phi=\Phi(X,z,T) \tag{2.5}$$

and let $R=R_0(1+\mu\epsilon^2)$. Since $0<\epsilon\ll1$, the scale of the motion is $O(1/\epsilon)$ in the original variables. With these variables Eqs. (2.1) become

$$\frac{1}{\sigma}\left[\epsilon^4\frac{\partial}{\partial T}(\epsilon^2\Psi_{XX}+D^2\Psi)+\epsilon^2\Psi_X(\epsilon^2D\Psi_{XX}+D^3\Psi)-\epsilon^2D\Psi(\epsilon^2\Psi_{XXX}+D^2\psi_X)\right]$$
$$=R_0(1+\mu\epsilon^2)(1+S)\epsilon^2\Theta_X+SR_0(1+\mu\epsilon^2)\Phi_X+\epsilon^4\Psi_{XXXX}+2\epsilon^2D^2\Psi_{XX}+D^4\Psi\ , \tag{2.6a}$$

$$\epsilon^4\frac{\partial\Theta}{\partial T}+\epsilon^2(\Psi_XD\Theta-D\Psi\Theta_X)=\Psi_X+\epsilon^2\Theta_{XX}+D^2\Theta\ , \tag{2.6b}$$

$$\epsilon^4\frac{\partial\Phi}{\partial T}+\epsilon^2(\Psi_XD\Phi-D\Psi\Phi_X)=\tau(\epsilon^2\Phi_{XX}+D^2\phi)-\epsilon^2(\epsilon^2\Theta_{XX}+D^2\Theta)\ . \tag{2.6c}$$

These equations can be solved by an asymptotic expansion of the form

$$\Psi=\Psi_0+\epsilon^2\Psi_2+\cdots\ ,$$
$$\Theta=\Theta_0+\epsilon^2\Theta_2+\cdots\ , \tag{2.7}$$
$$\Phi=\Phi_0+\epsilon^2\Phi_2+\cdots\ .$$

At leading order, Eq. (2.6c) yields

$$D^2\Phi_0=0, \quad \text{with } D\Phi_0=0 \quad \text{on } z=\pm1\ . \tag{2.8}$$

Hence

$$\Phi_0=f(X,T)\ . \tag{2.9}$$

From (2.6a) we have

$$D^4\Psi_0=-SR_0f'\ , \tag{2.10}$$

where the prime denotes $\partial/\partial X$, and hence

$$\Psi_0=SR_0f'P(z)\ . \tag{2.11}$$

Here the quartic polynomial $P(z)$ depend on the boundary conditions (2.3a)–(2.3c). From (2.6b) we similarly obtain

$$\Theta_0=SR_0f''Q(z)\ , \tag{2.12}$$

where the sextic polynomial $Q(z)$ depends not only on the boundary conditions (2.3d) and (2.3e), but through P also on (2.3a)–(2.3c).

At $O(\epsilon^2)$ we obtain from (2.6c),

$$\tau D^2\Phi_2=-(\tau+SR_0P)f''-SR_0DPf'^2\ . \tag{2.13}$$

In view of the boundary conditions (2.2), this equation has a solution if and only if

$$SR_0\int_{-1}^{1}P\,dz+2\tau=0\ . \tag{2.14}$$

This relation determines the critical Rayleigh number corresponding to the different boundary conditions (2.3a)–(2.3c). Note that the result is independent of the conditions (2.3d) and (2.3e). The corresponding solution of (2.13) takes the form

$$\Phi_2=f_2(X,T)+f''U(z)+f'^2V(z)\ , \tag{2.15}$$

where

$$D^2U=-\left[1+\frac{SR_0}{\tau}P\right],\quad D^2V=-\frac{SR_0}{\tau}DP\ . \tag{2.16}$$

Similarly,

$$\Psi_2=SR_0f_2'P(z)+\mu Sf'P(z)+f'f''W(z)+f'''Z(z)\ , \tag{2.17}$$

where

$$D^4W=\frac{1}{\sigma}(SR_0)^2(PD^3P-DPD^2P)-2SR_0V\ , \tag{2.18a}$$

$$D^4Z=-2SR_0D^2P-SR_0^2(1+S)Q-SR_0U\ . \tag{2.18b}$$

Moreover,

$$D^2\Theta_2=(SR_0)^2(f''^2PDQ-f'f'''DPQ)-SR_0f_2''P-\mu Sf''P-(f'f'')'W-f''''(Z+SR_0Q)\ . \tag{2.19}$$

Finally, at $O(\epsilon^4)$, the solvability condition for Φ_4 yields the desired evolution equation for f,

$$\frac{\partial f}{\partial T}=-R_0S\mu Af''-Bf''''+C(f'^3)'+D(f'f'')'\ , \tag{2.20}$$

where

$$A=-\tfrac{1}{2}\int_{-1}^{1}P\,dz\ , \tag{2.21a}$$
$$B=-\tfrac{1}{2}\left[\tau\int_{-1}^{1}U\,dz+\int_{-1}^{1}Z\,dz\right], \tag{2.21b}$$
$$C=\tfrac{1}{2}SR_0\int_{-1}^{1}DPV\,dz\ , \tag{2.21c}$$
$$D=\tfrac{1}{2}\left[2\tau\int_{-1}^{1}V\,dz+\int_{-1}^{1}W\,dz+SR_0\int_{-1}^{1}DPU\,dz+(SR_0)^2\int_{-1}^{1}DPQ\,dz\right]. \tag{2.21d}$$

In writing these expressions for the coefficients, we have used integration by parts, the boundary conditions $P(\pm1)=W(\pm1)=Z(\pm1)=0$ and the relation (2.14) to simplify the results. One important consequence is that the unknown function f_2 drops out and need not be determined. The coefficients A,B,C,D for various combinations of the boundary conditions (2.3a)–(2.3c) and (2.3d)–(2.3e) are listed in Table I. Note that $C>0$ always.

Equation (2.20) takes the same form as the corresponding equation for the Rayleigh-Bénard convection in a pure fluid with no-heat-flux boundary conditions at $z=\pm1$.[7,8] In particular, when both the stream function and thermal boundary conditions are the same at both top and bottom, the coefficient D vanishes and (2.20) is equivariant with respect to the symmetry $f\to-f$ inherited from a reflection symmetry in $z=0$. The resulting equation has been studied at length in Ref. 7 for $B>0$, and a roll of finite wave number was found to evolve continually towards smaller and smaller wave numbers. The most notable difference between the pure fluid problem and the present problem is that the coefficient B becomes negative for sufficiently small positive S. The value of S where this first happens, called S_∞ in Table I, is the smallest value of S at which the linear problem has $k_c=0$ as the mode that first becomes unstable. This is illustrated in Fig. 1 where the numerically calculated neutral curves for the boundary conditions (2.3b) and (2.3d) are shown for $S<S_\infty$, $S=S_\infty$, and $S>S_\infty$.[6] For $S>S_\infty$ the neutral curve has a minimum at $k=0$. Consequently the present method can be used to deduce analytically the values of S_∞ (cf. Fig. 8 of Ref. 6). Observe, finally, that in the case (2.3c) and (2.3e), the coefficient D can change sign as a function of the Lewis number τ.

The derivation of an evolution equation for two-dimensional patterns is complicated by the presence of vertical vorticity. However, when the Prandtl number $\sigma=\infty$, an assumption we henceforth make, the derivation of the corresponding evolution equation for the horizontal planform function $f(X,Y,T)$ is quite similar to that given above. Omitting the details we obtain

TABLE I. The critical Rayleigh number and the coefficients in Eq. (2.20) for various combinations of the boundary conditions (2.3a)–(2.3c) and (2.3d) and (2.3e). The value of the separation ratio S_∞ for which $B=0$ is also given.

Conditions	R_0	A	B	C	D	S_∞
(2.3a) and (2.3d)	$\frac{15}{2}\frac{\tau}{S}$	$\frac{2}{15}$	$-\frac{691}{1386}\left[1+\frac{1}{S}\right]\tau^2+\frac{1091}{1386}\tau$	$\frac{155\tau}{126}$	0	$\frac{691\tau}{1091-691\tau}$
(2.3b) and (2.3d)	$45\frac{\tau}{S}$	$\frac{1}{45}$	$-\frac{131}{231}\left[1+\frac{1}{S}\right]\tau^2+\frac{34}{231}\tau$	$\frac{10\tau}{7}$	0	$\frac{131\tau}{34-131\tau}$
(2.3c) and (2.3d)	$20\frac{\tau}{S}$	$\frac{1}{20}$	$-\frac{3280}{6237}\left[1+\frac{1}{S}\right]\tau^2+\frac{232}{693}\tau$	$\frac{760\tau}{567}$	$-\frac{\tau}{3}-\frac{5}{21}\frac{\tau^2}{\sigma}+\frac{\tau^2}{9}$	$\frac{410\tau}{261-410\tau}$
(2.3a) and (2.3e)	$\frac{15}{2}\frac{\tau}{S}$	$\frac{2}{15}$	$-\frac{2077}{1368}\left[1+\frac{1}{S}\right]\tau^2+\frac{1091}{1386}\tau$	$\frac{155\tau}{126}$	τ^2	$\frac{2077\tau}{1091-2077\tau}$
(2.3b) and (2.3e)	$45\frac{\tau}{S}$	$\frac{1}{45}$	$-\frac{362}{231}\left[1+\frac{1}{S}\right]\tau^2+\frac{34}{231}\tau$	$\frac{10\tau}{7}$	τ^2	$\frac{181\tau}{17-181\tau}$
(2.3c) and (2.3e)	$20\frac{\tau}{S}$	$\frac{1}{20}$	$-\frac{306}{231}\left[1+\frac{1}{S}\right]\tau^2+\frac{232}{693}\tau$	$\frac{760\tau}{567}$	$-\frac{\tau}{3}-\frac{5}{21}\frac{\tau^2}{\sigma}+\tau^2$	$\frac{459\tau}{116-459\tau}$

$$\frac{\partial f}{\partial t}=-R_0 S\mu A\nabla^2 f-B\nabla^4 f+C\nabla\cdot|\nabla f|^2\nabla f+\tfrac{1}{3}D(\nabla\cdot\nabla^2 f\nabla f+\nabla^2|\nabla f|^2)\,, \tag{2.22}$$

where $(X,Y)=\epsilon(x,y)$ are the appropriate slow variables in the horizontal, $\nabla\equiv(\partial/\partial X,\partial/\partial Y)$, and the coefficients A,B,C,D are given by (2.21). Equation (2.22) is very similar to (2.20); note, in particular, that $\frac{1}{3}(\nabla\cdot\nabla^2 f\nabla f+\nabla^2|\nabla f|^2)$ reduces to $(f'f'')'$ in the one-dimensional case. It can be shown that the structure of this term is a consequence of the self-adjointness of the linear problem.

In the above derivation the small parameter ϵ specifies the wave number of the pattern. When $B>0$ (i.e., $S>S_\infty$), this wave number is selected by nonlinear processes that are beyond the scope of the present paper. However, when $0<S_\infty-S\ll 1$, the quantity ϵ is related to the wave number at the *onset* of the instability and hence to the parameters of the linear theory allowing us to impose the wave number externally. Consequently, we focus in the following on analyzing (2.22) in a neighborhood of (R_0,S_∞) that is sufficiently small where that the above derivation still applies. This point is a type of codimension-two singularity for the present problem. Specifically, we let

$$S=S_\infty(1-\hat{\nu}\epsilon^2),\quad \hat{\nu}>0 \tag{2.23a}$$

$$R=R_0(1+\hat{\nu}\epsilon^2+\hat{\mu}\epsilon^4),\quad \hat{\mu}>\hat{\nu}^2\,. \tag{2.23b}$$

Then the linear terms in Eq. (2.22) both pick up a factor of ϵ^2. For consistency it is now necessary to scale $T\to T/\epsilon^2$ and either $f\to\epsilon^2 f$ (if $D\neq 0$) or $f\to\epsilon f$ (if $D=0$). This has the effect of introducing the term $\nabla^6 f$ into the evolution equation at leading order in ϵ. One obtains evolution equations of the form

$$\frac{\partial f}{\partial T}=-R_0 S_\infty(\hat{\mu}-\hat{\nu}^2)A\nabla^2 f+\hat{\nu}\hat{B}\nabla^4 f+F\nabla^6 f+\frac{D}{3}(\nabla\cdot\nabla^2 f\nabla f+\nabla^2|\nabla f|^2)\,, \tag{2.24a}$$

$$\frac{\partial f}{\partial T}=-R_0 S_\infty(\hat{\mu}-\hat{\nu}^2)A\nabla^2 f+\hat{\nu}\hat{B}\nabla^4 f+F\nabla^6 f+C\nabla\cdot|\nabla f|^2\nabla f\,, \tag{2.24b}$$

where $\hat{\nu}\hat{B}=B/\epsilon^2$. In these equations all the terms are formally of the same order. It is a simple matter to derive them from Eq. (2.1) given the above scalings. One then finds that

$$F=\tfrac{1}{2}\int_{-1}^{1}(L+H)\,dz\,, \tag{2.25}$$

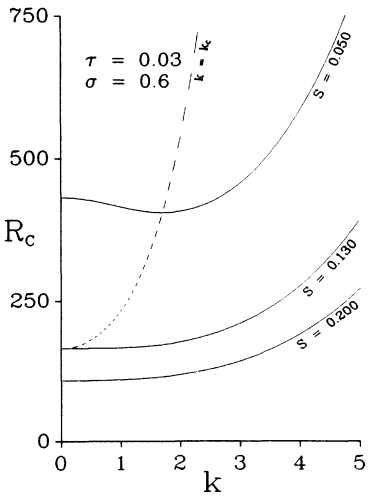

FIG. 1. Neutral stability curves $R_c(k)$ for the boundary conditions (2.3b) and (2.3d). The dashed line indicates the values of k_c which minimize $R_c(k)$ for each value of S. Note that k_c vanishes when $S\geq S_\infty\simeq 0.130$. After Ref. 6.

where

$$D^2L=-\tau U-Z\ , \tag{2.26a}$$

$$D^4H=-R_0(1+S_\infty)M - \left[\frac{R_0S_\infty}{\tau}\right]L-2D^2Z-R_0S_\infty P\ , \tag{2.26b}$$

$$D^2M=-R_0S_\infty Q-Z\ , \tag{2.26c}$$

with L, H, and M having the boundary conditions of Φ, Ψ, and Θ. Some tedious algebra readily shows that at the codimension-two point $(R,S)=(R_0,S_\infty)$, F is always positive, as already indicated by Fig. 1. For example, one finds that $F=0.095\tau$ for case (2.3b) and (2.3d) and $F=0.485\tau$ for case (2.3a) and (2.3d). Consequently we can scale out F by appropriately changing the units of X, Y and henceforth assume that this has been done.

In the following we shall find that neither equation (2.24) is completely satisfactory because of the presence of nongeneric behavior. For example, Eq. (2.24b) has the reflection symmetry $f\to -f$ which may be weakly broken. Consequently we focus here on the more general equation

$$\frac{\partial f}{\partial T}=-\mu\nabla^2 f+\nu\nabla^4 f+\nabla^6 f+\kappa\nabla\cdot|\nabla f|^2\nabla f + \frac{\beta}{3}(\nabla\cdot\nabla^2 f\nabla f+\nabla^2|\nabla f|^2)\ , \tag{2.27}$$

where the coefficients μ,ν,κ,β are related by an obvious transformation to those appearing in (2.24). Evidently, Eq. (2.27) includes both the possibilities (2.24) as special cases. However, it is more appropriate to think of (2.27) as arising from the scaling $f\to\epsilon f$, $D\to\epsilon D$, and $T\to T/\epsilon^2$. To make the coefficient D of order ϵ it is necessary to change the boundary conditions at $z=\pm 1$ and choose boundary conditions on the two plates that agree to within $O(\epsilon)$. For example, we can take the temperature to be fixed at $z=1$, i.e., $\theta=0$, and can suppose that due to constant power supplied to the bottom plate the appropriate thermal boundary condition there is $\epsilon D\theta+\theta=0$, where ϵ is now the inverse of the Biot number. With identical boundary conditions on ψ at the top and bottom this problem has $D=O(\epsilon)$. The analysis of the spatially periodic patterns described by Eq. (2.27) that begins in Sec. III shows that the symmetry-breaking terms ($\beta\neq 0$) have an important effect on the stability of the possible patterns in the present system.

III. PATTERN SELECTION ON THE SQUARE LATTICE

In this section we begin our study of pattern selection described by Eq. (2.27). The linearized equation has solutions of the form $\exp(st+i\mathbf{k}\cdot\mathbf{x})$, $\mathbf{x}\equiv(X,Y)$, where

$$s=k^2(\mu+\nu k^2-k^4)\ . \tag{3.1}$$

Hence the neutral stability curve $s=0$ has a minimum at $k=0$ when $\nu<0$, but when $\nu>0$, the minimum occurs at

$$\mu_c=-(\nu/2)^2,\quad k_c^2=\nu/2 \tag{3.2}$$

(cf. Fig. 1). To study pattern selection we look for solutions to (2.27) that are doubly periodic in the plane[11]

$$f(\mathbf{x})=f(\mathbf{x}+n_1\mathbf{a}_1+n_2\mathbf{a}_2)\ , \tag{3.3}$$

where n_1,n_2 are integers and the vectors $\mathbf{a}_i$ satisfy $\mathbf{a}_i\cdot\mathbf{k}_j=2\pi\delta_{ij}$, $|\mathbf{k}_j|=k_c$. This restriction to periodic solutions enables us to make use of the techniques of equivariant bifurcation theory. This is because at $\mu=\mu_c$ only a finite number of wave vectors are now marginally stable, and all remaining wave vectors have eigenvalues that are bounded away from zero. The vectors $\mathbf{a}_j$, or equivalently $\mathbf{k}_j$, define a two-dimensional lattice. Two cases are of interest. In the first the lattice has a square unit cell; the symmetry of the lattice is then the group $D_4\times T^2$, D_4 being the symmetry of the unit cell and the two-torus T^2 arising from translations (mod $2\pi/k_c$) in the directions $\mathbf{a}_1,\mathbf{a}_2$. In the second the unit cell is hexagonal, and the lattice symmetry is $D_6\times T^2$. In the following it will be important to observe that when $\beta=0$, Eq. (2.27) has the additional Z_2 symmetry generated by $f\to -f$. Consequently, the full symmetry of the problem is $D_4\times T^2\times Z_2$ and $D_6\times T^2\times Z_2$. However, since $D_4\times T^2\times Z_2\simeq D_4\times T^2$ (see Ref. 3) the extra reflection symmetry is important only on the hegagonal lattice.

In this section we study the square lattice. Here at $\mu=\mu_c$ the center eigenspace is spanned by vectors of the form[3]

$$f_0=\tfrac{1}{2}[z_1e^{ik_cX}+z_2e^{ik_cY}+\text{c.c.}\,|(z_1,z_2)\in\mathbb{C}^2]\ , \tag{3.4}$$

and for $\mu-\mu_c\equiv\lambda>0$ the amplitudes z_1,z_2 satisfy the equations[15]

$$\begin{pmatrix}\dot r_1\\ \dot r_2\end{pmatrix}=p\begin{pmatrix}r_1\\ r_2\end{pmatrix}+q\delta\begin{pmatrix}r_1\\ -r_2\end{pmatrix}\ , \tag{3.5a}$$

$$\dot\phi_1=\dot\phi_2=0\ . \tag{3.5b}$$

Here $z_j=r_j\exp i\phi_j$, $j=1,2$, and the real-valued functions p and q are functions of the invariants $N\equiv r_1^2+r_2^2$, $\Delta=\delta^2\equiv(r_2^2-r_1^2)^2$, and of λ. Existing results from singularity theory show that provided the nondegeneracy conditions

$$p_N(0)\neq 0,\quad q(0)\neq 0,\quad p_N(0)\neq q(0) \tag{3.6}$$

hold, the steady-state solutions of (3.5a) are in one-to-one correspondence with the zeros of the normal form[15]

$$n(r_1,r_2;\lambda)=(\lambda+mN)\begin{pmatrix}r_1\\ r_2\end{pmatrix}+\epsilon_0\delta\begin{pmatrix}r_1\\ -r_2\end{pmatrix},\quad m\neq 0,\epsilon_0\ , \tag{3.7}$$

where

$$\epsilon_0=\operatorname{sgn}[q(0)],\quad m=p_N(0)/|q(0)|\ , \tag{3.8}$$

and $p_N(0)$ denotes $\partial p/\partial N$ evaluated at $N=\Delta=\lambda=0$, etc. The analysis of the normal form (3.7) shows that there are two nontrivial zeros, $(r_1,r_2)=(r_R,0)$ and $(r_1,r_2)=(r_S,r_S)$, corresponding to rolls and squares, respectively. The normal form (3.7) can also be used to

determine the stability of these solutions with respect to perturbations on the square lattice.[3,15] One finds that rolls are stable if $p_N(0)-q(0)<0$, $q(0)<0$, while squares are stable if $p_N(0)<0$, $q(0)>0$.

To calculate the coefficients $p_N(0)$, $q(0)$ we employ standard perturbation theory, writing

$$f=\epsilon f_0+\epsilon^2 f_1+\epsilon^3 f_2+\cdots , \tag{3.9a}$$

$$\mu=\mu_c+\epsilon\mu_1+\epsilon^2\mu_2+\cdots , \tag{3.9b}$$

and seek steady-state solutions of (2.27) in the form

$$f(X,Y)=r_1\cos(k_c X)+r_2\cos(k_c Y) . \tag{3.10}$$

At each order we determine μ_n from a solvability condition for the problem

$$L_0 f_n=-\sum_{j=0}^{n-1}\mu_{n-j}\nabla^2 f_j+F(f_0,\ldots,f_{n-1}) , \tag{3.11}$$

where $L_0\equiv -k_c^4\nabla^2-2k_c^2\nabla^4-\nabla^6$ and F denotes nonlinear terms. At $O(\epsilon^2)$ we find $\mu_1=0$, while at $O(\epsilon^3)$ we obtain the two conditions

$$[\mu_2-\tfrac{1}{2}\kappa k_c^2(\tfrac{3}{2}r_1^2+r_2^2)-\beta^2(\tfrac{1}{4}r_1^2+\tfrac{1}{2}r_2^2)]r_1=0 , \tag{3.12a}$$

$$[\mu_2-\tfrac{1}{2}\kappa k_c^2(\tfrac{3}{2}r_2^2+r_1^2)-\beta^2(\tfrac{1}{4}r_2^2+\tfrac{1}{2}r_1^2)]r_2=0 \tag{3.12b}$$

by eliminating from the right-hand side of (3.11) terms of the form $\cos(k_c X)$ and $\cos(k_c Y)$, respectively. From these results we deduce that the branches of rolls and squares bifurcate simultaneously from $\mu=\mu_c$ with their directions of branching given by

$$\mu_2^R=(\tfrac{3}{4}\kappa k_c^2+\tfrac{1}{4}\beta^2)r_R^2 , \tag{3.13a}$$

$$\mu_2^S=(\tfrac{5}{4}\kappa k_c^2+\tfrac{3}{4}\beta^2)r_S^2 . \tag{3.13b}$$

Since $\kappa>0$ it follows that both rolls and squares bifurcate supercritically with increasing μ.

If we compare these results with those obtained from a Taylor expansion of the vector field (3.5a) we readily obtain

$$\frac{q(0)}{p_\lambda(0)}=\tfrac{1}{8}(\kappa k_c^2-\beta^2) , \tag{3.14a}$$

$$\frac{p_N(0)}{p_\lambda(0)}=-\tfrac{1}{8}(5\kappa k_c^2+3\beta^2) , \tag{3.14b}$$

where $p_\lambda(0)=k_c^2>0$. Hence, when

$$\kappa k_c^2=\beta^2 , \tag{3.15}$$

the nondegeneracy condition $q(0)\neq 0$ fails, and we have a degenerate or codimension-two bifurcation. This bifurcation separates the two cases $\kappa k_c^2>\beta^2$ (squares stable) and $\kappa k_c^2<\beta^2$ (rolls stable), shown in Fig. 2. Note that squares are stable provided the boundary conditions at the top and bottom are not too different. Note also that as S approaches S_∞ from below, k_c tends to zero, so that condition (3.15) occurs for smaller and smaller values of β. Thus in this limit the region of stable squares shrinks to zero.

The nature of the transition between stable squares and

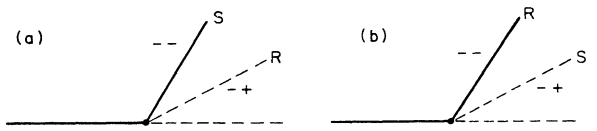

FIG. 2. Bifurcation diagrams $N(\lambda)$ on the square lattice for (a) $\beta<k_c$ and (b) $\beta>k_c$. The stability of rolls (R) and squares (S) is indicated by the signs of the eigenvalues: negative (stable), positive (unstable). Solid lines denote stable branches.

stable rolls can be studied analytically near the codimension-two degeneracy $\mu=\mu_c, k_c^2=\beta^2$, where we have set, without loss of generality, $\kappa=1$. Singularity theory[16] shows that in this case the zeros of the vector field (3.5a) are in one-to-one correspondence with those of the normal form

$$n(r_1,r_2;\lambda,\alpha)=(\lambda+\epsilon_1 N+\epsilon_2\Delta)\begin{bmatrix} r_1 \\ r_2 \end{bmatrix} +(\alpha+N)\delta\begin{bmatrix} r_1 \\ -r_2 \end{bmatrix} , \tag{3.16}$$

where

$$\begin{aligned}\epsilon_1&=\mathrm{sgn}[p_N(0)] ,\\ \epsilon_2&=\mathrm{sgn}[q_N(0)p_\Delta(0)-q_\Delta(0)p_N(0)] ,\end{aligned} \tag{3.17}$$

and λ,α are the two unfolding parameters, proportional to $\mu-\mu_c$ and $q(0)$, respectively. The vector field (3.16) is a normal form provided the two nondegeneracy conditions

$$p_N(0)\neq 0, \quad q_N(0)p_\Delta(0)-q_\Delta(0)p_N(0)\neq 0 \tag{3.18}$$

hold at the degeneracy. Analysis of the zeros of (3.16) and their stability shows that if $\alpha<0$, there is a branch of steady-state solutions of the form $(r_1,r_2), r_1\neq r_2$, hereafter referred to as crossrolls (CR), which bifurcates in secondary pitchfork bifurcations from the S and R branches, and is stable when $\epsilon_1<0$, $\epsilon_2>0$ and unstable when $\epsilon_1<0, \epsilon_2<0$. In the present case, $\epsilon_1=-1$ since $p_N(0)<0$ [Eq. (3.14b)], and it remains to calculate ϵ_2 to determine the nature of the transition from stable squares to stable rolls. Note that since $p_\Delta(0)$ and $q_N(0)$ are coefficients of fifth-order terms in (3.5a) while $q_\Delta(0)$ is a coefficient of a seventh-order term, it is necessary to go to seventh order in the calculation that follows.[17] Essentially identical conclusions follow from a singularity theory analysis in which λ is treated as a distinguished parameter.[16]

To calculate these coefficients we carry expansion (3.9) to seventh order. The calculation is done at the degenerate bifurcation point. With $\kappa=1$ we therefore set

$$\mu=\mu_c, \quad \beta=k_c . \tag{3.19}$$

At $O(\epsilon^4)$ we obtain no solvability condition, while at $O(\epsilon^5)$ we find that the following two conditions hold:[18]

$$(\tfrac{1}{64}r_1^4-\tfrac{851}{1440}r_1^2r_2^2+\tfrac{139}{180}r_2^4)r_1=0 , \tag{3.20a}$$

$$(\tfrac{139}{180}r_1^4-\tfrac{851}{1440}r_1^2r_2^2+\tfrac{1}{64}r_2^4)r_2=0 . \tag{3.20b}$$

These conditions are to be identified with the fifth-order terms in the vector field (3.5)

$$\frac{1}{p_\lambda(0)}\{[\tfrac{1}{2}p_{NN}(0)+p_\Delta(0)-q_N(0)]r_1^4+[p_{NN}(0)-2p_\Delta(0)]r_1^2r_2^2+[\tfrac{1}{2}p_{NN}(0)+p_\Delta(0)+q_N(0)]r_2^4\}r_1=0\ , \tag{3.21a}$$

$$\frac{1}{p_\lambda(0)}\{[\tfrac{1}{2}p_{NN}(0)+p_\Delta(0)+q_N(0)]r_1^4+[p_{NN}(0)-2p_\Delta(0)]r_1^2r_2^2+[\tfrac{1}{2}p_{NN}(0)+p_\Delta(0)-q_N(0)]r_2^4\}r_2=0\ . \tag{3.21b}$$

We deduce that

$$\begin{aligned} p_{NN}(0)&=0.0984p_\lambda(0)\ ,\\ p_\Delta(0)&=0.3447p_\lambda(0)\ ,\\ q_N(0)&=0.3783p_\lambda(0)\ . \end{aligned} \tag{3.22}$$

Note that (3.20) by themselves do not admit solutions with $r_1\neq r_2$. The crossrolls are present in the *unfolding* of (3.20) only. At $O(\epsilon^6)$ there is again no solvability condition. Finally, at $O(\epsilon^7)$ we obtain

$$(0.0067r_1^6+3.831r_1^4r_2^2+2.927r_1^2r_2^4-1.237r_2^6)r_1=0\ , \tag{3.23a}$$

$$(-1.237r_1^6+2.927r_1^4r_2^2+3.831r_1^2r_2^4+0.0067r_2^6)r_2=0\ , \tag{3.23b}$$

and conclude that

$$\begin{aligned} p_{NNN}(0)&=4.145p_\lambda(0)\ ,\\ p_{N\Delta}(0)&=-1.306p_\lambda(0)\ ,\\ q_{NN}(0)&=-1.159p_\lambda(0)\ ,\\ q_\Delta(0)&=-0.0425p_\lambda(0)\ , \end{aligned} \tag{3.24a}$$

It follows that $\epsilon_2=1$. Since $\lambda\equiv\mu-\mu_c$ and $\alpha=\frac{1}{8}(k_c^2-\beta^2)$, we now know all the coefficients in the normal form (3.16). The results of the corresponding analysis are summarized in Fig. 3.[16] For $\beta<k_c$ [Fig. 3(a)] the initial instability gives rise to a pattern of squares which remain stable with increasing Rayleigh number μ. For $\beta>k_c$ [Fig. 3(b)] the initial instability develops into a pattern of rolls. As μ increases the rolls lose stability at a secondary pitchfork bifurcation producing a branch of crossrolls. This branch is stable and terminates on the branch of squares in another pitchfork bifurcation. At this bifurcation the squares acquire stability and remain the stable solution for yet larger μ. Thus stability is transferred from rolls to squares via a secondary branch of crossrolls. This completes our discussion of the bifurcations on the square lattice.

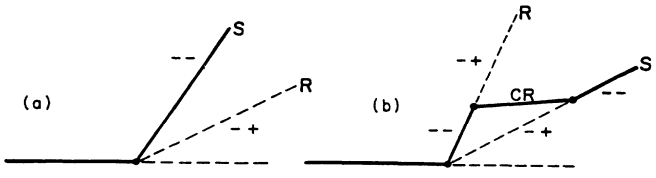

FIG. 3. Bifurcation diagrams $N(\lambda)$ near the codimension-two degeneracy for (a) $0<k_c-\beta\ll 1$, and (b) $0<\beta-k_c\ll 1$. In (b) stability is transferred from rolls to squares via a stable branch of cross rolls.

IV. PATTERN SELECTION ON THE HEXAGONAL LATTICE

On the hexagonal lattice the center eigenspace at $\mu=\mu_c$ is spanned by vectors of the form[3,11]

$$f_0=\tfrac{1}{2}[z_1e^{ik_cX}+z_2e^{ik_c(\sqrt{3}Y-X)/2}+z_3e^{-ik_c(\sqrt{3}Y+X)/2}+\text{c.c.}(z_1,z_2,z_3)\in\mathbb{C}^3]\ . \tag{4.1}$$

We consider first the case $\beta=0$. Then Eq. (2.27) has the additional reflection symmetry $f\to -f$, and symmetry considerations lead to the following equations for the amplitudes (z_1,z_2,z_3):[3,11]

$$\dot{z}_1=z_1(l_1+u_1l_3+u_1^2l_5)+\bar{z}_2\bar{z}_3q(m_5+u_1m_7+u_1^2m_9) \tag{4.2}$$

together with the equations obtained by cyclic permutation of (z_1,z_2,z_3). Here the quantities l_j,m_j are real-valued functions of $\sigma_1,\sigma_2,\sigma_3$ and q^2 given by

$$\sigma_1=u_1+u_2+u_3\ , \tag{4.3a}$$

$$\sigma_2=u_1u_2+u_2u_3+u_3u_1\ , \tag{4.3b}$$

$$\sigma_3=u_1u_2u_3\ , \tag{4.3c}$$

$$q=z_1z_2z_3+\bar{z}_1\bar{z}_2\bar{z}_3\ , \tag{4.3d}$$

where $u_j=z_j\bar{z}_j$, $j=1,2,3$, and of the bifurcation parameter $\lambda\equiv\mu-\mu_c$.

In Table II we list the six types of steady solutions that are of interest to the present problem. The table lists the representatives from the fixed-point subspaces of each solution type together with the terminology that will be used to refer to them. In the generic case, studied in Ref. 11, the following nondegeneracy conditions are assumed to hold:

$$\begin{aligned} &l_{1,\sigma_1}(0)+l_3(0)\neq 0\ ,\\ &2l_{1,\sigma_1}(0)+l_3(0)\neq 0\ ,\\ &3l_{1,\sigma_1}+l_3(0)\neq 0\ , \end{aligned} \tag{4.4a}$$

$$l_3(0)\neq 0,\quad m_5(0)\neq 0\ . \tag{4.4b}$$

Under these conditions four primary branches bifurcate simultaneously from the trivial solution at $\mu=\mu_c$. These are rolls (R), patchwork quilt (PQ), hexagons (H) and regular triangles (RT) (see Table II); of these PQ can never be stable. However, in the present problem $l_3(0)\equiv 0$. To show this we determine perturbatively the roll and hexagon branches. We find that

TABLE II. The six most important solution types to Eqs. (4.2).

Pattern	(z_1,z_2,z_3)	Conditions	Abbreviation
Rolls	$\hat{x}(1,0,0)$	$\hat{x}>0$	R
Hexagons	$\hat{x}(1,1,1)$	$\hat{x}>0$, $\hat{x}<0$	H^+,H^-
Patchwork quilt	$\hat{x}(0,1,1)$	$\hat{x}>0$	PQ
Rectangles	$\hat{x}\left[1,\frac{1}{a},\frac{1}{a}\right]$	$\hat{x}>0$, $a\neq 0,1,\infty$	RA
Regular triangles	$\hat{y}(i,i,i)$	$\hat{y}>0$	RT
Imaginary rectangles	$\hat{y}\left[i,\frac{i}{a},\frac{i}{a}\right]$	$\hat{y}>0$, $a\neq 0,1,\infty$	IRA

$$\mu_2^R=-\frac{l_{1,\sigma_1}(0)+l_3(0)}{l_{1,\lambda}(0)}\hat{x}_R^2=\tfrac{3}{4}\kappa k_c^2\hat{x}_R^2\ , \tag{4.5a}$$

$$\mu_2^H=-\frac{3l_{1,\sigma_1}(0)+l_3(0)}{l_{1,\lambda}(0)}\hat{x}_H^2=\tfrac{9}{4}\kappa k_c^2\hat{x}_H^2\ . \tag{4.5b}$$

Since $l_{1,\lambda}(0)=k_c^2$, we therefore have

$$l_{1,\sigma_1}(0)=-\tfrac{3}{4}\kappa k_c^4<0\ , \tag{4.6a}$$

$$l_3(0)=0\ . \tag{4.6b}$$

The degeneracy (4.6b) has a number of important consequences.[12] Specifically as many as six primary solution branches can now bifurcate simultaneously at $\mu=\mu_c$. These are the solutions listed in Table II. Since $l_{1,\sigma_1}(0)<0$, all bifurcate supercritically. To determine their relative stability, i.e., stability with respect to perturbations on the hexagonal lattice, it is necessary to determine three fifth-order terms in the Taylor expansion of (4.2). The results of the abstract theory[12] are summarized in Fig. 4, showing the $(l_{3,\sigma_1}(0),l_5(0))$ plane for $m_5(0)>0$. The plane splits into 12 regions with distinct bifurcation diagrams. In the insets we show which of the six possible solutions exist in which region, and list the nonzero eigenvalues characterizing their stability. The stable patterns are explicitly indicated in each of the 12 regions. It will be observed that in each at least one pattern is stable, with stable rolls and hexagons coexisting in regions 2, 3, and 12, and stable hexagons and patchwork quilts coexisting in regions 8 and 9. Neither rectangles nor imaginary rectangles can ever be stable.

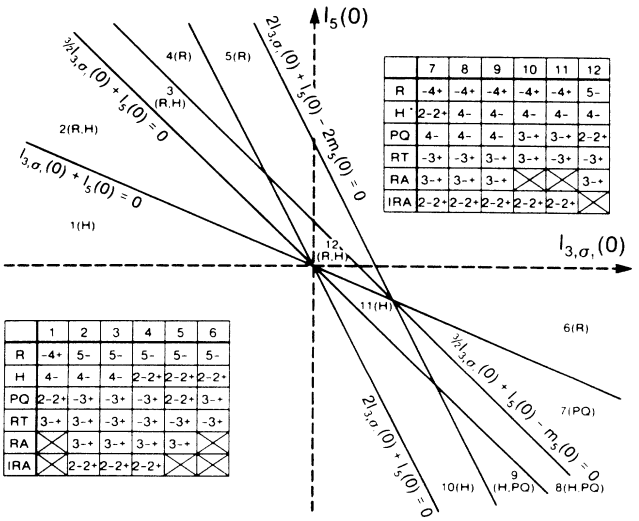

	7	8	9	10	11	12
R	-4+	-4+	-4+	-4+	-4+	5-
H	2-2+	4-	4-	4-	4-	4-
PQ	4-	4-	4-	3-+	3-+	2-2+
RT	-3+	-3+	3-+	3-+	-3+	-3+
RA	3-+	3-+	3-+			3-+
IRA	2-2+	2-2+	2-2+	2-2+	2-2+	

	1	2	3	4	5	6
R	-4+	5-	5-	5-	5-	5-
H	4-	4-	4-	2-2+	2-2+	2-2+
PQ	2-2+	-3+	-3+	-3+	2-2+	3-+
RT	3-+	3-+	-3+	-3+	-3+	-3+
RA		3-+	3-+	3-+	3-+	
IRA		2-2+	2-2+	2-2+		

FIG. 4. The $(l_{3,\sigma_1}(0),l_5(0))$ plane for $m_5(0)>0$, showing the 12 regions in which distinct bifurcation diagrams occur. The inset tables give the number of negative (stable) and positive (unstable) eigenvalues for each of the solution branches present in each region. The stable pattern(s) in each region is (are) indicated explicitly. After Ref. 12.

To use this classification it is necessary to determine the three coefficients $l_{3,\sigma_1}(0)$, $l_5(0)$, and $m_5(0)$. We first note from (4.2) that the hexagon and RT branches are given by

$$l_{1,\lambda}(0)\lambda+3\hat{x}_H^2 l_{1,\sigma_1}(0)+\hat{x}_H^4[\tfrac{9}{2}l_{1,\sigma_1\sigma_1}(0)+3l_{1,\sigma_2}(0)+3l_{3,\sigma_1}(0)+l_5(0)+2m_5(0)]+O(6)=0\ , \tag{4.7a}$$

$$l_{1,\lambda}(0)\lambda+3\hat{y}_{\mathrm{RT}}^2 l_{1,\sigma_1}(0)+\hat{y}_{\mathrm{RT}}^4[\tfrac{9}{2}l_{1,\sigma_1\sigma_1}(0)+3l_{1,\sigma_2}(0)+3l_{3,\sigma_1}(0)+l_5(0)]+O(6)=0\ . \tag{4.7b}$$

Hence by computing hexagons and RT to fourth order we determine the coefficient $m_5(0)$. It is also possible to show from (4.2) that the RA branch exists provided[12]

$$[l_{3,\sigma_1}(0)+l_5(0)]a_{\mathrm{RA}}^2+2l_{3,\sigma_1}(0)+l_5(0)-2m_5(0)=O(2)\ , \tag{4.8a}$$

while the IRA branch exists provided

$$[l_{3,\sigma_1}(0)+l_5(0)]a_{\mathrm{IRA}}^2+2l_{3,\sigma_1}(0)+l_5(0)=O(2)\ . \tag{4.8b}$$

Note that the parameter a is uniquely specified. This is a consequence of the fact that $l_3(0)$ vanishes identically, and thus cannot become an unfolding parameter. In more general circumstances the RA and IRA solutions would have two-dimensional fixed-point subspaces. From the results (4.8) it follows that if we determine the value of a^2 for the RA and IRA branches, we obtain two independent relations between $l_{3,\sigma_1}(0)$ and $l_5(0)$. Together with $m_5(0)$ this provides sufficient information to determine the three fifth-order coefficients.[18]

A. Rectangles

To find a solution of Eq. (2.27) in the form of RA we use perturbation theory starting with the linear result (4.1) with $(z_1,z_2,z_3)=\hat{x}_{\rm RA}(1,1/a,1/a)$. At second order in the amplitude $\hat{x}_{\rm RA}$, we find

$$\mu_2^{\rm RA}=\tfrac{3}{4}\kappa k_c^2\left[1+\frac{2}{a^2}\right]\hat{x}_{\rm RA}^2 . \tag{4.9}$$

Note that when $a=1$, this reduces to the result (4.5b) for hexagons, and when $a=\infty$, it reduces to the result (4.5a) for rolls. The result (4.9) holds for any a. This is no longer true at fourth order in $\hat{x}_{\rm RA}$, where one obtains two solvability conditions,

$$\mu_4^{\rm RA}+\left[\frac{3}{64}+\frac{15}{14a^2}+\frac{93}{56a^4}\right]\frac{\hat{x}_{\rm RA}^4}{16}=0 , \tag{4.10a}$$

$$\frac{\mu_4^{\rm RA}}{a}+\frac{1}{a}\left[\frac{15}{56}+\frac{93}{56a^2}+\frac{381}{448a^4}\right]\frac{\hat{x}_{\rm RA}^4}{16}=0 , \tag{4.10b}$$

from which it follows that

$$\mu_4^R=-\tfrac{3}{1024}\hat{x}_R^4 , \tag{4.11a}$$

$$\mu_4^H=-\tfrac{1245}{7168}\hat{x}_H^4 . \tag{4.11b}$$

The corresponding results for PQ can be obtained by taking the limit $a\to 0$ with $\hat{x}/a$ fixed, but are not required in what follows. In addition, by eliminating $\mu_4^{\rm RA}$ from (4.10) we obtain the value of a^2 on the RA branch,

$$3a^2+11=0,\quad a\neq 0,1,\infty . \tag{4.12}$$

Since a has to be real, this result implies that the RA branch does not, in fact, exist. Nonetheless this result can be used in (4.8a) to obtain the relation

$$5l_{3,\sigma_1}(0)+8l_5(0)+6m_5(0)=0 . \tag{4.13}$$

B. Imaginary rectangles

A similar procedure for solutions in the form of IRA yields at second order in $\hat{y}_{\rm IRA}$ a relation identical to (4.9). At fourth order in $\hat{y}_{\rm IRA}$ we obtain

$$\mu_4^{\rm IRA}+\left[\frac{3}{64}+\frac{15}{14a^2}-\frac{33}{56a^4}\right]\frac{\hat{y}_{\rm IRA}^4}{16}=0 , \tag{4.14a}$$

$$\frac{\mu_4^{\rm IRA}}{a}+\frac{1}{a}\left[\frac{15}{56}-\frac{3}{112a^2}+\frac{129}{448a^4}\right]\frac{\hat{y}_{\rm IRA}^4}{16}=0 . \tag{4.14b}$$

Setting $a=\infty$, we recover the result (4.11a) for rolls; for RT we find

$$\mu_4^{\rm RT}=-\tfrac{237}{7168}\hat{y}_{\rm RT}^4 . \tag{4.15}$$

Finally, solving (4.14) for a^2 along the IRA branch shows that

$$33a^2-131=0,\quad a\neq 0,1,\infty . \tag{4.16}$$

Hence the IRA branch does exist; Eq. (4.8b) yields the relation

$$197l_{3,\sigma_1}(0)+164l_5(0)=0 . \tag{4.17}$$

If we now use the results (4.11b) and (4.15) in (4.7), we can determine the coefficient $m_5(0)$,

$$m_5(0)=\tfrac{9}{32}k_c^2>0 . \tag{4.18}$$

Moreover, from (4.13) and (4.17) we deduce

$$l_{3,\sigma_1}(0)=\tfrac{41}{112}k_c^2,\quad l_5(0)=-\tfrac{197}{448}k_c^2 . \tag{4.19}$$

We conclude, therefore, that the present system falls in region 11 of Fig. 4, and that hexagons are the stable pattern, with the remaining four patterns, rolls, PQ, RT, and IRA, all unstable.

When $\beta\neq 0$ the midplane reflection symmetry is absent. In this case equations (4.2) are replaced by

$$\dot{z}_1=z_1(h_1+u_1h_3+u_1^2h_5)+\bar{z}_2\bar{z}_3(p_2+u_1p_4+u_1^2p_6) , \tag{4.20}$$

where the quantities h_j,p_j are now real-valued functions of σ_1, σ_2, σ_3, q, and λ. One must now distinguish between H^+ ($\hat{x}_H>0$) and H^- ($\hat{x}_H<0$). When $p_2(0)\neq 0$, one can easily show that there are only three primary branches, rolls and hexagons (H^+,H^-), which bifurcate simultaneously at μ_c and that all are locally unstable.[11] In the present problem, owing to the self-adjointness of the operator L, $p_2(0)=0$, and there are *four* primary branches, rolls, hexagons (H^+,H^-), and rectangles.[11]

This bifurcation problem is described by the normal form

$$n_1\equiv z_1(\lambda+a\sigma_1+eu_1+d\sigma_1^2)+\bar{z}_2\bar{z}_3(b\sigma_1+u_1+cq)=0 , \tag{4.21}$$

analyzed in Ref. 11. The analysis shows that if $e>0$ and $a+e<0$, rolls are stable regardless of the various higher-order terms. We now show that this is the case in the present problem. To do this we calculate the hexagon branch to second order in the amplitude, obtaining

$$\mu_2^H=(\tfrac{9}{4}\kappa k_c^2+\beta^2)x_H^2 . \tag{4.22}$$

Thus, since $\kappa>0$, $\mu_2^4>0$ and both hexagon branches bifurcate supercritically. From the normal form (4.21) we have, however,

$$\lambda=-(a+\tfrac{1}{3}e)\sigma_1+O(\sigma_1^2) \tag{4.23a}$$

for hexagons and

$$\lambda=-(a+e)\sigma_1+O(\sigma_1^2) \tag{4.23b}$$

for rolls. It follows from (3.10a) and (4.22) that

$$a+\tfrac{1}{3}e=-\tfrac{3}{4}\kappa k_c^2-\tfrac{1}{3}\beta^2 , \tag{4.24a}$$

$$a+e=-\tfrac{3}{4}\kappa k_c^2-\tfrac{1}{4}\beta^2 . \tag{4.24b}$$

Since $e=\beta^2/8>0$ and $a+e<0$, we conclude that rolls are stable with respect to perturbations on the hexagonal

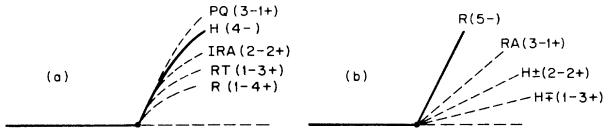

FIG. 5. Bifurcation diagrams $\sigma_1(\lambda)$ on the hexagonal lattice for (a) $\beta=0$ and (b) $\beta\neq 0$. In (a) there are five primary branches of which hexagons are stable; in (b) there are four branches of which rolls are stable.

lattice (see Fig. 5). Thus hexagons are stable only in the special case $\beta=0$.

V. DISCUSSION AND CONCLUSION

This paper was motivated by a desire to understand the types of transitions between squares and rolls that can occur in binary-fluid mixtures heated from below. Since it is well known that the boundary conditions, and, in particular, the no-mass-flux boundary condition, are essential for such an understanding, we selected a separation ratio regime $0<S_\infty-S\ll 1$ in which the wavelength of the initial instability is long, though finite, and the basic equations can be reduced to an evolution equation for the horizontal planform only. Such an equation can be derived for a great variety of boundary conditions, including any that are of experimental interest, and requires no approximation. We have found that an important role is played by the lack of symmetry in the boundary conditions at the top and bottom, and found that the small amplitude dynamics of the system can be fully captured by analyzing a system with slight asymmetry only.

In order to understand the transition between squares and rolls we studied pattern selection on the square lattice. This procedure, appropriate for large-aspect-ratio systems, showed that with symmetric or nearly symmetric boundary conditions squares are indeed stable, at least with respect to perturbations on the square lattice, in agreement with the suggestion made in Ref. 2. We found, however, that if a small asymmetry is present then squares will be replaced by rolls as S approaches closer and closer to S_∞ from below. To elucidate the nature of this instability we studied a particular codimension-two bifurcation. The analysis showed that the rolls are stable at small amplitudes only. As the Rayleigh number is increased the rolls lose stability at a secondary pitchfork bifurcation producing a *stable* branch of crossrolls. This branch, in turn, terminates on the branch of squares, which thereby gain stability. Thus the squares remain the preferred pattern at larger Rayleigh numbers even with substantial asymmetry in the boundary conditions. Consequently the analysis is unable to describe the transition from squares to rolls that is observed in the experiments at $R-R_0=O(1)$.

We also carried out a similar analysis on the hexagonal lattice. Here the symmetric problem was found to be degenerate. Consequently, as many as six primary branches could bifurcate simultaneously from the trivial solution. We have determined that of these the hexagonal pattern is the only pattern that is stable with respect to perturbations on the hexagonal lattice. In addition, we showed that with an asymmetry, however small, in the boundary conditions at top and bottom the hexagons lose stability to rolls.

Taken together these results suggest that squares will be stable near onset for $0<\beta<k_c$ while rolls will be stable for $\beta>k_c$. However, no such conclusion can be drawn about the special case $\beta=0$. The prevalence of stable squares in the nearly symmetric case suggests in turn that an exact treatment, along the lines of Ref. 3, of binary-fluid convection with smaller values of S would also yield stable squares. Together with the fact that experiments in circular,[1] square,[2] and rectangular[2] containers all reveal stable squares near onset, these results suggest that side-wall forcing is unnecessary for the existence of stable squares. The possibility remains, however, that the oscillations observed at larger amplitude are affected by the side walls, and additional experiments on the influence of side walls are clearly desirable.

In view of the role played in the pattern selection process by the asymmetry in the boundary conditions at the top and bottom of the layer, it is important to observe that small non-Boussinesq terms also break the up-down symmetry. However, as discussed elsewhere,[19] these terms break in addition the self-adjointness of the linear stability problem and so have a qualitatively distinct effect. On the square lattice, squares remain stable when these terms are sufficiently small; with increasing non-Boussinesq terms, squares bifurcate subcritically but acquire stability at a secondary saddle-node bifurcation. On the hexagonal lattice, no stable patterns are produced by the primary bifurcation, although hexagons (either H^+ or H^-, depending on the sign of the non-Boussinesq term) acquire stability in a secondary saddle-node bifurcation; when $\beta=0$ the other hexagon branch also acquires stability but in a secondary bifurcation producing an unstable branch of triangles.[19] On the other hand, when $\beta\neq 0$ rolls become stable at larger amplitude. Thus when the non-Boussinesq terms are small their effect is confined to the vicinity of the primary bifurcation.

In conclusion, we note that with stress-free boundary condition oscillations may also arise from a coupling to a mean flow of strength $O(\epsilon^5)$, required by Galilean invariance.[20] The evolution equation for such a flow requires perturbation theory to $O(\epsilon^{11})$. Only then would it be possible to describe the resulting oscillatory instability of the finite-amplitude patterns found above.

ACKNOWLEDGMENTS

The author is grateful to Professor Y. Kuramoto for his kind hospitality in Kyoto where most of this work was done, and to the Japan Society for the Promotion of Science for financial support. Very helpful correspondence with Dr. M. R. E. Proctor is also acknowledged.

*On leave from the Department of Physics, University of California, Berkeley, California 94720.

[1]P. LeGal, A. Pocheau, and V. Croquette, Phys. Rev. Lett. **54**, 2501 (1985).

[2]E. Moses and V. Steinberg, Phys. Rev. Lett. **57**, 2018 (1986); V. Steinberg and E. Moses, in *Patterns, Defects and Microstructures,* in *NATO Advanced Study Institute, Series B: Physics* (Martinus Nijhoff, Hingham, MA, 1987), pp. 309–335.

[3]M. Silber and E. Knobloch, Phys. Rev. A **38**, 1468 (1988).

[4]H. W. Müller, and M. Lücke, Phys. Rev. A **38**, 2965 (1988).

[5]D. A. Nield, J. Fluid Mech. **29**, 545 (1967); *ibid.* **71**, 441 (1975); D. Gutkowicz-Krusin, M. A. Collins, and J. Ross, Phys. Fluids **22**, 1443 (1979); G. W. Lee, P. Lucas, and A. Tyler, J. Fluid Mech. **135**, 235 (1983); B. J. A. Zielinska and H. R. Brand, Phys. Rev. A **35**, 4349 (1987); **37**, 1786(E) (1988).

[6]E. Knobloch and D. R. Moore, Phys. Rev. A **37**, 860 (1988).

[7]C. J. Chapman and M. R. E. Proctor, J. Fluid Mech. **101**, 759 (1980).

[8]V. L. Gertsberg and G. I. Sivashinsky, Prog. Theor. Phys. **66**, 1219 (1981).

[9]M. C. Depassier and E. A. Spiegel, Geophys. Astrophys. Fluid Dyn. **21**, 167 (1982).

[10]D. Hefer and L. M. Pismen, Phys. Fluids **30**, 2648 (1987).

[11]M. Golubitsky, J. W. Swift, and E. Knobloch, Physica D **10**, 249 (1984); M. Silber and E. Knobloch, *ibid.* **30**, 83 (1988) and Ref. 3.

[12]E. Knobloch (unpublished).

[13]E. Knobloch, Phys. Rev. A **34**, 1538 (1986).

[14]E. M. Sparrow, R. J. Goldstein, and V. K. Jonsson, J. Fluid Mech. **18**, 513 (1964); E. Jakeman, Phys. Fluids **11**, 10 (1968).

[15]M. Golubitsky and I. Stewart, Arch. Rat. Mech. Anal. **87**, 107 (1985); Ref. 3.

[16]J. D. Crawford and E. Knobloch, Physica **31D**, 1 (1988); the distinguished parameter classification by M. Golubitsky and M. Roberts, J. Diff. Eq. **69**, 216 (1987), is not used in the present paper.

[17]E. Knobloch, Contemp. Math. **56**, 193 (1986).

[18]More detail concerning such calculations may be found in Ref. 12.

[19]E. Knobloch, in *Cooperative Dynamics in Complex Systems,* Proceedings of the Second Yukawa International Seminar, Kyoto, Japan, 1988, edited by H. Takayma (Springer-Verlag, Berlin, in press).

[20]P. Coullet and S. Fauve, Phys. Rev. Lett. **55**, 2857 (1985).